RSC Advances

ROYAL SOCIETY OF CHEMISTRY

www.rsc.org/advances

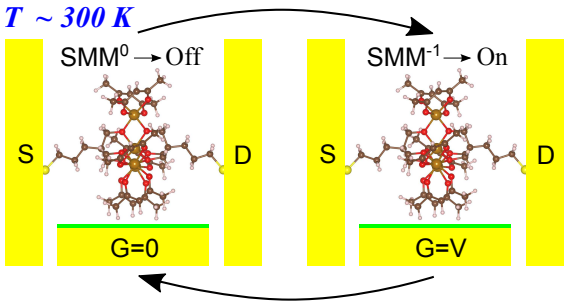

Figure 1 Table Of Contents: Based on charge-state transition, a molecular memory device of single-molecule magnets can work even at room temperature.

Journal Name

ARTICLE TYPE

Cite this: DOI: 10.1039/xxxxxxxxxx

Room temperature memory device using single-molecule magnets

Hua Hao,[a,b] XiaoHong Zheng,[a,b] Ting Jia, [a,b]and Zhi Zeng[a,b,c,*]

Received Date
Accepted Date

DOI: 10.1039/xxxxxxxxxx

www.rsc.org/journalname

To make memory devices of an individual single-molecule magnet work far above blocking temperature, we propose a new route, where the information is contained in the charge state of the molecule, and it works on charging and discharging the molecule by applying gate voltages. Here, a model device built on a single-molecule magnet Fe_4 is taken as example to exhibit the validity of our proposed route. *Ab*-initio calculations show that the two different charge states with a moderately large energy shift of 1.2 eV are responsible for the low and high conductances in this device: one corresponds to the neutral state of the molecule, and the other to its anionic state. Moreover, the transition from the neutral state to the anionic state is accompanied by a giant increase of nearly two orders of magnitude in the conductance. Additionally, the low and high conductances before and after charging the molecule are hardly dependent on different spin configurations of the Fe_4 molecule, which indicates that the performance of the Fe_4 memory device is probably preserved even at room temperature.

1 Introduction

In molecular spintronics[1–3], single-molecule magnets (SMMs) have attracted great interests due to their outstanding chemical characteristics and impressive magnetic properties[4]. Particularly, SMMs' magnetization relaxation time is extremely long below their blocking temperature (T_B)[5]. As a result, a memory device can be constructed using SMMs, where the information is contained in the magnetization direction of SMMs, and the on /off states are achieved by switching their magnetization direction. Nevertheless, SMMs' blocking temperature mostly remains in the liquid-helium temperature range ($\sim$ 4 K)[6], in spite of great efforts for improving SMMs' magnetic properties[7–12]. Such a low blocking temperature possibly causes the paramagnetic state of SMMs in practical environments[13,14], and the memory device based on the magnetization direction of SMMs may fail to work, since the ambient temperature is generally far above the liquid-helium temperature or even in the room-temperature range. Consequently, new working mechanisms are necessary to build practical memory devices using SMMs.

In this work, we propose an alternative route to greatly raise the working temperature of a SMM-based molecular memory device. In this memory device, two different charge states are concerned to represent the low and high conductances, and the device works on charging and discharging the central molecule by applying gate voltages. Here, we take a model device of a SMM Fe_4[15–17] as an example to show the performance of the memory device based on the charge-state transition. Numerical calculations demonstrate that the low and high conductances of the Fe_4 memory device can be denoted by the neutral state and the anionic state of the molecule, and the conductance difference between the two charge states reaches two orders of magnitude. Moreover, the switching between the high and

[a] *Key Laboratory of Materials Physics, Institute of Solid State Physics, Chinese Academy of Sciences, Hefei 230031, China.*
[b] *University of Science and Technology of China, Hefei, 230026, China.*
[c] *Beijing Computational Science Research Center, Beijing 100084, China.*
[*] *Email: zzeng@theory.issp.ac.cn; Fax: +86-551-65591434; Tel: +86-551-65591407.*

† Electronic Supplementary Information (ESI) available: [details of any supplementary information available should be included here]. See DOI: 10.1039/b000000x/

‡ Additional footnotes to the title and authors can be included *e.g.* 'Present address:' or 'These authors contributed equally to this work' as above using the symbols: ‡, §, and ¶. Please place the appropriate symbol next to the author's name and include a `\footnotetext` entry in the the correct place in the list.

low conductances is hardly achieved by thermal perturbations ($\sim$ 26 meV at room temperature) and low bias voltages ($\leq$ 0.16 eV), since the charge-state transition is closely associated with a moderately large energy shift of 1.2 eV. Further studies reveal that the low and high conductances before and after charging the Fe_4 molecule are independent of spin configurations (magnetic states) of the SMM Fe_4. Base on these facts, the Fe_4 memory device can work far above its blocking temperature or even at room temperature. The rest of this paper describes our calculations and results in greater details.

2 Computational details

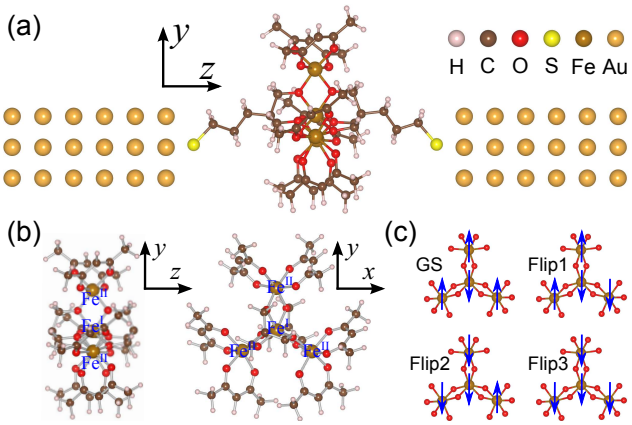

Fig. 1 (color online). (a) the structure of the model device: an individual Fe_4 is sandwiched between two Au(100) nano-electrodes. z denotes the electron transport direction. Different atoms are distinguished by different colors. (b) the magnetic core of the Fe_4 molecule at different angles. The central Fe^{3+} ion is named Fe^{I}, and the three equivalent peripheral Fe^{3+} ions are named Fe^{II}. (c) different spin configurations for the Fe_4 molecule. The arrows denote the spin directions of Fe^{3+} ions.

The model Fe_4 device is displayed in Fig. 1 (a), in which the sulphur-functionalized Fe_4 molecule is connected to two semi-infinite nano-scale Au(100) electrodes. For the Fe_4 molecule, the 3-fold symmetry[18] leads to two nonequivalent Fe^{3+} ions: one is the central Fe^{3+} ion marked by Fe^{I} in Fig. 1 (b); the other is the peripheral Fe^{3+} ion marked by Fe^{II}. Four spin configurations depicted in Fig. 1 (c) are consider in this work: the ground spin configuration (GS) and three excited spin flip configurations (Flip1, Flip2, Flip3). The parallel (antiparallel) arrows mean the ferromagnetic (antiferromagnetic) coupling between the Fe^{3+} ions. The nano-electrodes have been adopted by many authors in the study of molecular devices[19–21]. A large enough vacuum layer around the electrode in the x and y direction is chosen so that the device has no interactions with its mirror images. Electron transport properties are calculated using the SMEAGOL program[22], which combines the non-equilibrium Green's function approach with the density functional theory calculations implemented in the SIESTA code[23,24]. The capability of the code has been well verified to treat electron transport properties of SMMs[25,26]. Specifically, the exchange-correlation potential takes the form of the Ceperley-Alder parameterization of the local density approximation[27]. Only valence electrons are self-consistently calculated, and the atomic cores are described by scalar relativistic norm-conserving pseudopotential[28]. The valence wave functions are expanded by localized numerical atomic orbitals[29] and the basis set is constructed as follows: SZP for Au and DZ for other atoms (SZ=single-ζ, DZ=double-ζ, and P=Polarized). Molecular structures are fully relaxed until the force tolerance is reached at 0.03 eV/Å. It is pointed out that although spin-polarized calculations are performed to correctly simulate different spin configurations of Fe_4, only the total transmission and current are necessary and presented in this paper.

3 Results and Discussion

In the neutral state of the ground spin configuration (or GS-NS), Fig. 2 (a) shows that the electron transmission is quite weak near the Fermi level ($\sim 10^{-6}$). To understand the negligible transmission, the local density of states (LDOS) is calculated by the formula $n(E,\vec{r},\sigma) = \int |\psi_\sigma(\vec{r})|^2 \delta(E-\varepsilon_\sigma) dE$ integrated over (-0.1, 0.1 eV), where E is the energy, $\vec{r}$ is the spatial coordinates, σ is the spin, and $\psi_\sigma(\vec{r})$ is an eigenstate with eigenenergy ε_σ. This quantity returns the spatially resolved density of states in a molecular device, and allow one to know which atoms in space are contributing to electron tunnelling. From the LDOS displayed by the inset of Fig. 2 (a), it is found that electronic states for electron tunneling are only distributed on Au electrodes and S-Au interfaces near the Fermi level, but totally absent in the magnetic-core region of the Fe_4 molecule. Obviously, the absence of electronic states in such a region is responsible for the poor transmission near the Fermi level in the Fe_4 device. By analyzing the projected density of states (PDOS) displayed in Fig. 2 (b), it is noted that electronic states of the nano-electrodes are distributed over the whole energy range (-1.6, 1.6 eV), however, the lowest unoccupied molecular orbital (LUMO) of the Fe_4 molecule is 1.2 eV above the Fermi level, and its highest occupied molecular orbital (HOMO) is 1.0 eV below the Fermi level. It is well known that electron transmission from one electrode to the other in a molecular device must be meditated by a certain molecular orbital. Hence, the poor transmission around the Fermi level fundamentally arises from the fact that both HOMO and LUMO are far away from the Fermi level in this device. In a word, a low conductance or the off state can be denoted by the GS-NS.

To acquire a high conductance or the on state in the Fe_4 memory device, a certain gate voltage [$V_G = 3.0$ V] is applied on the magnetic-core region of the Fe_4 molecule [Fig. 1 (b)], and the molecule is then charged by nearly one electron. For such an

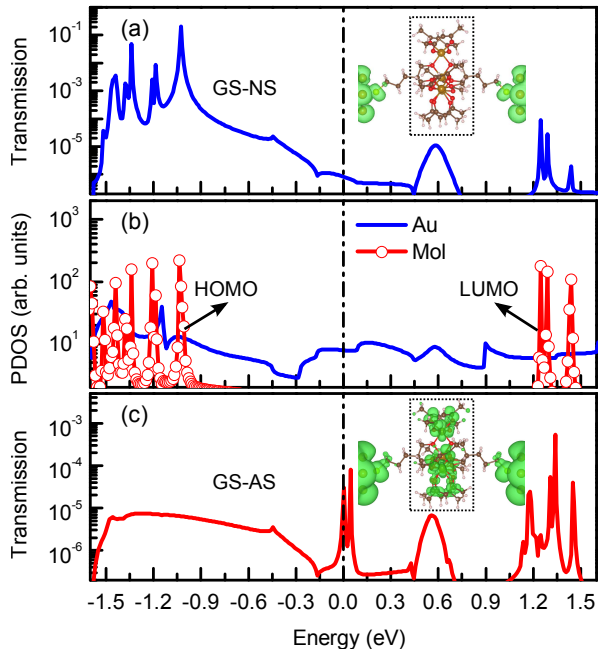

Fig. 2 (color online). (a) the total transmission spectrum of the neutral state in the ground spin configuration (GS-NS); (b) the projected density of states for the Fe_4 devices in the GS-NS; (c) the total transmission spectrum of the anionic state in the ground spin configuration (GS-AS). The insets in (a) and (c) show the local density of states for the Fe_4 devices integrated from -0.1 to 0.1 eV with isosurface criterion of $0.1e/nm^3$. Au and Mol in (b) denote the Au nano-electrodes and the Fe_4 molecule; HOMO and LUMO denote the highest occupied molecular orbital and the lowest unoccupied molecular orbital.

anionic state of the ground spin configuration (or GS-AS), some electronic states are observed around the Fermi level, in addition to electronic states from Au electrodes and S-Au interfaces, by analyzing the LDOS [the inset of Fig. 2 (c)]. These electronic states naturally result in a transmission peak near the Fermi level in Fig. 2 (c), with the magnitude of nearly 10^{-4}. As a result, the transmission in the GS-AS is about two orders of magnitude larger than that of the GS-NS ($\sim 10^{-6}$), which is consistent with the notable increase in the conductance in the experiment[17]. As a matter of fact, the gate-induced anionic states are always associated with the appearance of some unoccupied molecular orbitals around the Fermi level. Obviously, the LUMO is the direct origin of the transmission peak near the Fermi level for the GS-AS with only one extra electron. As a whole, a high conductance or the on state is achieved in the GS-AS obtained by applying a gate voltage.

The above results clearly exhibit that the high and low conductances required by a memory device can be accomplished by charging and discharging the Fe_4 molecule. Moreover, it is noted that the LUMO is actually 1.2 eV above the Fermi level in the GS-NS, which indicates that the switching between off state and on state can hardly be realized by thermal perturbations (~ 26 meV at room temperature) and low bias voltages (≤ 0.16 V). According to these results, it seems that the Fe_4 memory device can work above the blocking temperature of the Fe_4 molecule or even at room temperature. Nevertheless, up to now, only the ground spin configuration has been considered in the above results. To guarantee the Fe_4 memory device workable above the blocking temperature, it is very important to study excited spin configurations of the Fe_4 molecule which will appear above the blocking temperature, and see whether the conductance switching is still observable in these excited spin configurations.

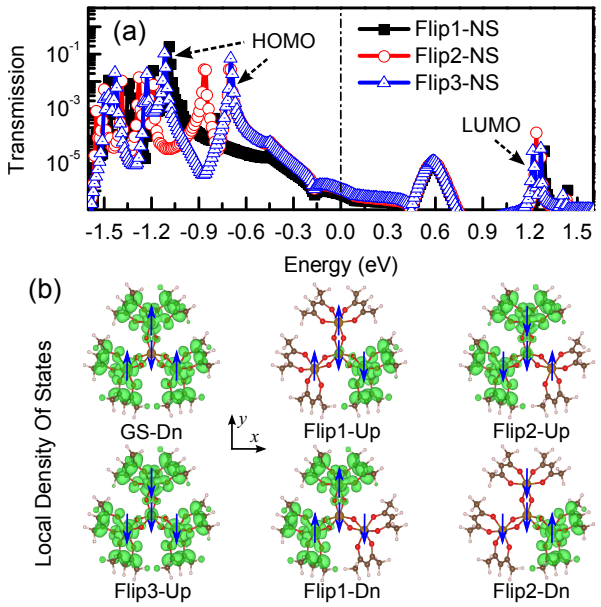

Fig. 3 (color online). (a) the total transmission spectra in the neutral state of three excited spin configurations (Flip1-NS, Flip2-NS, and Flip3-NS). HOMO and LUMO denote the transmission peaks generated by electron tunneling through the highest occupied molecular orbital and the lowest unoccupied molecular orbital. (b) the local density of states for the lowest unoccupied molecular orbital for the four considered spin configurations with isosurface criterion of $1e/nm^3$. Some atoms are removed for clarity, on which none of electronic states are distributed.

Three excited spin flip configurations marked by 'Flip1', 'Flip2' and 'Flip3' in Fig. 1 (c) are respectively considered in the neutral state and the anionic state. The total energy of the Flip1 (Flip2, Flip3) spin configuration is about 17 (34, 51) meV higher than that of the GS in the experiment[18]. It is pointed out that the four considered spin configurations only differ in spin directions or magnetic couplings of the Fe^{3+} ions, while the spin quantum number of the Fe^{3+} ion is kept the same as $S = 5/2$. Under these three excited spin configurations, the HOMO and LUMO are similarly far away from the Fermi level, as described in Fig. 3 (a), thus the poor transmission near the Fermi level is still observed in the neutral state of these excited spin configurations

(Flip1-NS, Flip2-NS, and Flip3-NS). This fact proves that the low conductance is independent on spin configurations of the Fe_4 molecule. More interestingly, we note that the LUMO is found to be all about 1.2 eV above the Fermi level in the neutral state of the four considered spin configurations [see Fig. 2 (a) and Fig. 3 (a)], which implies that the LUMOs of the four considered spin configurations should share some features in common. This predication is verified by analyzing the LDOS of the LUMO presented in Fig. 3 (b). In the GS-NS, the LUMO totally lies in the spin-down branch and the corresponding charge distribution is mostly around the three peripheral Fe^{3+} ions. In the Flip1-NS (Flip2-NS), although the LUMO is split into two spin branches, they are degenerate in energy and the total charge distribution of the LUMO is negligibly different from that of the GS-NS. In the Flip3-NS, the charge distribution of the LUMO is also quite close to that of the GS-NS, except for different spin branches. The similar charge distributions of the LUMOs basically guarantee that the high conductance in the anionic state is also independent on spin configurations of the Fe_4 molecule. Further calculations confirm that when the same gate voltage [$V_G = 3.0$ V] is applied, the transmission peak arising from electron tunneling through the LUMO also appears near the Fermi level in the anionic state of three excited spin configurations (Flip1-AS, Flip2-AS, and Flip3-AS), and their transmission magnitudes are all around 10^{-4}. Consequently, the high conductance is also proven to be independent on spin configurations of the Fe_4 molecule. Incidentally, the energy positioning of the HOMO is found to be greatly dependent on spin configurations of the Fe_4 molecule [see Fig. 2 (a) and Fig. 3 (a)], which is the reason why the HOMO or the cationic state is not chosen to generate the on state of the Fe_4 device.

Furthermore, non-equilibrium transport properties are also examined under a bias voltage ranging from 0.02 V to 0.16 V, which is far away from the Coulomb blockade. The current is approximately 0.002 nA in the neutral state for the four considered spin configurations, as displayed in Fig. 4 (a). In the anionic state, the current can generally jump to around 0.2 nA, when a certain bias voltage (≥ 0.08 V) is applied. To quantify this notable increase in the conductance, we define a conductance increase ratio as $(G_{AS}\text{-}G_{NS})/G_{AS}$. The value of such a ratio can reach nearly 100 for the four considered spin configurations [see Fig. 4 (b)], accompanied by the charge-state transition. Accordingly, the low and high conductances required by a memory device can be denoted by these two charge states even under bias voltages, and they are also independent on spin configurations of the Fe_4 molecule.

It is pointed out that our proposed route can be applied to building high-temperature memory devices (or memory devices working far above blocking temperature) using other SMMs, as long as the molecular structures are highly symmetric in the

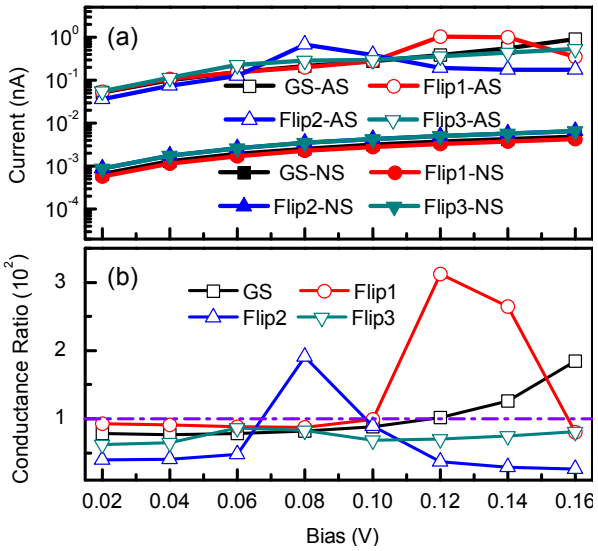

Fig. 4 (color online). (a) I-V curves in the neutral state and the anionic state for the four considered spin configurations. (b) the conductance increase ratio of the four considered spin configurations under bias.

transport direction and the ground charge states are greatly retained when they are anchored on a metallic surface, but is not limited to the SMM Fe_4. Besides, although magnetic properties of SMMs are used in our proposed memory device, SMMs are still good candidates for building such devices, since their chemical characteristics are superior to those of other molecules (see Ref. 4). For example, SMMs consist of an inner core with a surrounding shell of organic ligands. The surrounding ligands can be tailored to strongly bind SMMs on surfaces or into junctions. Meanwhile, their electron transport properties generally dependent on the inner cores can be preserved in different device environments due to the protection of the surrounding ligands. This probably makes one easily enhance the robustness of the device performance, which is one important merit for practical applications. Moreover, SMMs allow selective substitutions of the ligand (or metallic ions) to alter the coupling to the environment (or their physical properties without modifying the structure or coupling), which is another merit for rationally building practical molecular devices.

4 Conclusion

In conclusion, we propose a memory device of an individual SMM Fe_4, which works on charging and discharging the Fe_4 molecule by applying gate voltages. Numerical calculations show that the switching between the neutral state and the anionic state leads to a change of nearly two orders of magnitude in the conductance. Moreover, the LUMO, responsible for the high conductance in the anionic state, is found to be 1.2 eV above the Fermi level in the neutral state, thus the low and high conductances are well

separated even considering the thermal perturbations (~ 26 meV) and low bias voltages (≤ 0.16 V). Importantly, it is proven that different spin configurations of the SMM Fe_4 have little impact on the performance of the memory device. According to the above facts, the proposed Fe_4-based memory device can work far above its blocking temperature or even at room temperature.

ACKNOWLEDGEMENTS

This work was supported by the National Science Foundation of China under Grant Nos. 11104277, 11374301, 11174289, 11204309, and U1230202 (NSAF), the special Funds for Major State Basic Research Project of China (973) under Grant No. 2012CB933702, Hefei Center for Physical Science and Technology under Grant no. 2012FXZY004 and Director Grants of CASHIPS. The calculations were performed in Center for Computational Science of CASHIPS, the ScGrid of Supercomputing Center and Computer Network Information Center of Chinese Academy of Science.

References

1 S. Sanvito, Chem. Soc. Rev. **40**, 3336-3355 (2011).

2 W. Y. Kim, Y. C. Choi, S. K. Min, Y. Cho, and K. S. Kim, Chem. Soc. Rev. **38**, 2319-2333 (2009).

3 A. R. Rocha, V. M. García-suárez, S. W. Bailey, C. J. Lambert, J. Ferrer, and S. Sanvito, Nature Mater. **4**, 335-339 (2005).

4 L. Bogani and W. Wernsdorfer, Nature Mater. **7**, 179-186 (2008), and references therein.

5 The blocking temperature of SMMs is defined as the temperature below which the relaxation time of the magnetization becomes much longer than the time scale of an investigation technique, or the highest temperature at which magnetic hysteresis is observed. Its value is closely associted with the energy barrier $\Delta E = -DS^2$ (D, axial zero-field splitting parameter; S, the total spin number). Generally, larger $|\Delta E|$ indicates higher blocking temperature.

6 D. Gatteschi and A. Vindigni, arXiv:1303.3731. [cond-mat.str-el]

7 N. F. Chilton, C. A. P. Goodwin, D. P. Mills, and R. E. P. Winpenny, Chem. Commun. **51** 101 (2015).

8 E. Burzurí, R. Gaudenzi, and H. S. J. van der Zant, Journal of Physics: Condensed Matter **27**, 113202 (2015).

9 R. A. Layfield, Organometallics **33**, 1084-1099 (2014).

10 S. Gangopadhyay, A. E. Masunov, and S. Kilina, J. Phys. Chem. C **118**, 20605-20612 (2014).

11 J. D. Rinehart, M. Fang, W. J. Evans, and J. R. Long, J. Am. Chem. Soc. **133**, 14236-14239 (2011).

12 S. Gangopadhyay, A. E. Masunov, E. Poalelungi, and M. N. Leuenberger, J. Chem. Phys. **132**, 244104 (2010).

13 M. Cavallini, M. Facchini, C. Albonetti, and F. Biscarini, Phys. Chem. Chem. Phys. **10**, 784 (2008).

14 N. Baadji and S. Sanvito, Phys. Rev. Lett. **108**, 217201 (2012).

15 M. Mannini, F. Pineider, P. Sainctavit, C. Danieli, E. Otero, C. Sciancalepore, A. M. Talarico, M.-A. Arrio, A. Cornia, D. Gatteschi, and R. Sessoli, Nature Mater. **8**, 194 (2009).

16 A. S. Zyazin, J. W. G. van den Berg, E. A. Osorio, H. S. J. van der Zant, N. P. Konstantinidis, M. Leijnse, M. R. Wegewijs, F. May, W. Hofstetter, C. Danieli, and A. Cornia, Nano. Lett. **10**, 3307 (2010).

17 E. Burzurí, A. S. Zyazin, A. Cornia, and H. S. J. van der Zant, Phys. Rev. Lett. **109**, 147203 (2012).

18 S. Accorsi, A.-L. Barra, A. Caneschi, G. Chastanet, A. Cornia, A. C. Fabretti, D. Gatteschi, C. Mortalò, E. Olivieri, F. Parenti, P. Rosa, R. Sessoli, L. Sorace, W. Wernsdorfer, and L. Zobbi, J. Am. Chem. Soc. **128**, 4742-4755 (2006).

19 J. Taylor, H. Guo, and J. Wang, Phys. Rev. B **63**, 121104 (2001).

20 B. Larade, J. Taylor, Q. R. Zheng, H. Mehrez, P. Pomorski, and H. Guo, Phys. Rev. B **64**, 195402 (2001).

21 H. Hao, X. H. Zheng, Z. X. Dai, and Z. Zeng, Appl. Phys. Lett. **96**, 192112 (2010).

22 A. R. Rocha, V. García-Suárez, S. W. Bailey, C. J. Lambert, J. Ferrer, and S. Sanvtio, Phys. Rev. B **73**, 085414 (2006); I. Rungger and S. Sanvito, Phys. Rev. B **78**, 035407 (2008).

23 J. M. Soler, E. Arcacho, J. D. Gale, A. García, J. Junquera, P. Ordejón, and D. Sánchez-Portal, J. Phys.: Condens. Matter **14**, 2745-2779, (2002); E. Artacho, E. Anglada, O. Diéguez, J. D. Gale, A. García, J. Junquera, R. M. Martin, P. Ordejón, J. M. Pruneda, and J. M. Soler, J. Phys.: Condensed Matter, **20**, 064208 (2008).

24 E. Arcacho, J. D. Gale, A. García, J. Junquera, R. M. Martin, P. Ordejón, D. Sánchez-Portal, J. M. Soler, *Siesta*, Madrid, http://departments.icmab.es/leem/siesta/.

25 C. D. Pemmaraju, I. Rungger, and S. Sanvito, Phys. Rev. B **80**, 104422 (2009).

26 K. Park, S. Barraza-Lopez, V. M. García-Suárez, and J. Ferrer, Phys. Rev. B **81**, 125447 (2010).

27 D. M. Ceperley and B. J. Alder, Phys. Rev. Lett. **45**, 566 (1980).

28 N. Troullier and J. L. Martins, Phys. Rev. B **43**, 1993-2006 (1991).

29 E. Artacho, D. Sánchez-Portal, P. Ordejón, A. Grcía, and J. M. Soler, Phys. Status Solidi B **215**, 809-817 (1999).